Tree Physiology 00, 1–17
https://doi.org/10.1093/treephys/tpad007

Research paper

Modeling starch dynamics from seasonal variations of photosynthesis, growth and respiration

Scott W. Oswald[1,2,3] and Doug P. Aubrey[1,2]

[1]Savannah River Ecology Lab, Savannah River Site, Jackson, Bldg. 737-A, Aiken, SC 29802, USA; [2]Warnell School of Forestry and Natural Resources, University of Georgia, 180 E Green Street, Athens, Ga 30602-2152, USA; [3]Corresponding author (scott.oswald25@uga.edu)

Received June 13, 2022; accepted January 20, 2023; handling Editor Simon Landhäusser

Nonstructural carbohydrates (NSCs) buffer differences in plant carbon supply (photosynthesis) and demand (respiration, growth, etc.), but the regulation of their dynamics remains unresolved. Seasonal variations in NSCs are well-documented, but differences in the time-average, amplitude, phase and other characteristics across ecosystems and functional types lack explanation; furthermore, observed dynamics do not always match expectations. The failure to match observed and expected dynamics has stimulated debate on whether carbon supply or demand drives NSC dynamics. To gain insight into how carbon supply and demand drive seasonal NSC dynamics, we derive a simple model of NSC dynamics based on carbon mass balance and linearizing the NSC demand to determine how supply-driven and demand-driven seasonal NSC dynamics differ. We find that supply-driven and demand-driven dynamics yield distinct timings of seasonal extrema, and supply overrides demand when carbon supply is low in winter (e.g., at high latitudes). Our results also suggest that NSC dynamics often lag changes carbon mass balance. We also predict differences in NSC dynamics across mass, suggesting that saplings are more dynamic and respond more quickly to the environment than mature trees. Our findings suggest that substrate-dependent regulation with environmental variation is sufficient to generate complex NSC dynamics.

Keywords: active storage, carbon limitation, carbon reserves, demand, dynamics, regulation, supply.

Introduction

Plants drive the terrestrial carbon cycle (Bonan 2008). For terrestrial ecosystems, plant photosynthesis represents the principal source of carbon and free energy (Chapin et al. 2011). The study of plant physiological responses thus provides insights into how ecosystems will respond to climate change. Despite strong mechanistic descriptions of photosynthetic responses to its environmental drivers (Farquhar et al. 1980, Von Caemmerer 2013), the same for growth, carbon storage or carbon allocation remains lacking (Hartmann and Trumbore 2016, Fatichi et al. 2019). Uncertainty in plant physiological responses is a major source of uncertainty for terrestrial ecosystem carbon cycle models (Arora et al. 2013, Friedlingstein et al. 2014) appearing to result from differences in model structure (Lovenduski and Bonan 2017, Quetin and Swann 2018); these discrepancies suggest that models fail to capture important feedbacks or regulatory mechanisms in long-term responses. For instance, free-air CO_2 enrichment (FACE) studies find that these models correctly predict increased photosynthesis but not necessarily increased growth, typically because of nitrogen limitation (Nowak et al. 2004, Norby and Zak 2011). Nonstructural carbohydrates (NSCs) mediate the decoupling of photosynthesis and the rest of plant metabolism (Aubrey et al. 2012, Aubrey and Teskey 2018, Ruswick et al. 2021). Describing the dynamics of NSCs will elucidate the nature of this decoupling.

Sugars and starch, collectively NSCs, are the stable products of photosynthesis, requiring no nutrients to synthesize, unlike biosynthesis for growth or secondary metabolites. Photosynthesis need not equal growth, respiration and other aspects of plant metabolism at short timescales because change in NSCs buffers the difference. Photosynthesis only determines the supply of NSCs but not the demand for NSCs in metabolism. Growth, respiration and other processes together form the

demand for NSCs and therefore only depend on photosynthesis indirectly through their combined effect on the amount of NSCs. Nonstructural carbohydrate concentrations vary temporally in many observations. For instance, NSC concentrations oscillate over the course of each year in many species, but these seasonal variations differ in time-average, maximum, minimum, and when the maximum and minimum occur across organs, species or functional groups, latitude and climate (Richardson et al. 2013, Martínez-Vilalta et al. 2016, Davidson et al. 2021). Seasonal variations in NSC concentrations likely reflect seasonal changes in plant carbon balance that is asynchrony between supply and demand (Hartmann and Trumbore 2016), but the exact nature of this relationship remains contested. Differences in the observed dynamics of sugars and starch, and differences in temporal dynamics across plant organs have also remained difficult to fully explain. In fact, sugars play many roles beyond storage (e.g., biosynthesis, osmoregulation, phloem transport), and their variations may not reflect carbon balance while starch dynamics do.

The nature of the regulation of NSC dynamics remains a major knowledge gap for plant carbon dynamics (Chapin et al. 1990, Kozlowski 1992, Landsberg 2003, Körner 2015, Hartmann et al. 2020), and the exact nature of storage's role in plant carbon dynamics also remains contested (Sala et al. 2012, Dietze et al. 2014, Körner 2015, Hartmann and Trumbore 2016, Fatichi et al. 2019, Hartmann et al. 2020). See Sala et al. (2012), Dietze et al. (2014) or Hartmann and Trumbore (2016) for recent reviews. The debate centers on whether NSC regulation is passive or active (Wiley and Helliker 2012, Dietze et al. 2014) and whether plant growth is source or sink limited (Körner 2015, Fatichi et al. 2019). The latter relates to the former because carbon supply minus demand (e.g., growth) equals the change in NSCs regardless of why supply or demand increased or decreased. Some authors interpret large stocks or seasonal increases in NSCs as evidence of non-photosynthetic controls on growth such as nitrogen limitation, water limitation or temperature-dependent changes (Körner 2003, 2015, Woodruff and Meinzer 2011, Fatichi et al. 2014, Woodruff 2014), and thus they interpret observed NSC dynamics as evidence of sink-limited growth. This interpretation explains the lack of consistent growth responses to CO_2 enrichment studies despite increased photosynthesis, contrary to source-limited growth (Ainsworth and Long 2005). Other authors suggest that NSC demand may be regulated to maintain NSCs at a certain level, refilling NSC reserves preferentially over supporting growth when reserves are depleted (Sala et al. 2012, Wiley and Helliker 2012, Dietze et al. 2014). These different frameworks for NSC regulation lead to differing interpretations of the same observed dynamics; while they have motivated many experiments, the basic questions posed by these previous works remain incompletely answered.

Although not formulated in mathematical terms, many researchers have studied these conceptualizations of NSC dynamics via mathematical modeling. Nonstructural carbohydrate dynamics have long been present in plant physiological models (e.g., Thornley 1970, 1971), but due to the recent interest in NSCs, new works have implemented versions of NSC regulation or sink-limited growth models (exploring the latter is more common than the former), often with an eye toward the improvement of dynamic global vegetation models (Leuzinger et al. 2013, Schiestl-Aalto et al. 2015, 2019, Hayat et al. 2017, Jones et al. 2020, Potkay et al. 2022). Many carbon allocation models often also imply certain forms of NSC dynamics, even if not directly modeled (see reviews, e.g., Cannell and Dewar 1994, Le Roux et al. 2001, Franklin et al. 2012). While such models contain useful insights into NSC dynamics, the complexity of their formulation, along with the difficulty of parameterization, hinders analyzing their structure and applying them to experiments.

Despite the accumulation of experiments and models, the basic science of NSC regulation has received few significant refinements in 30 years (Chapin et al. 1990, Fatichi et al. 2019); this slow advance could indicate the need for a shift in perspective. Experiments and models of NSC dynamics have focused on the large number of environmental factors influencing these dynamics (Richardson et al. 2013, Schiestl-Aalto et al. 2015; Dietze et al. 2016; Hartmann and Trumbore 2016, Martínez-Vilalta et al. 2016, Jones et al. 2020, Davidson et al. 2021); however, this focus neglects the role of internal feedbacks, which may instead form the basis of regulation. As precedent, consider the classic idea that feedbacks between carbon and nitrogen substrate limitation ultimately drive carbon allocation (Thornley 1972); while the environment influences allocation, the regulation results from the presence of feedbacks. The mathematical study of dynamical systems supports this viewpoint. The importance of substrate dependence by NSCs on NSC demands alone, especially on respiration, is also a classic idea (Thornley 1970, 1971), and it has experimental support (e.g., Högberg et al. 2001, Sevanto et al. 2014, Collins et al. 2021). Many models of NSC dynamics make similar assumptions about how the amount of NSC stored affects its rate of change (e.g., Thornley 2011, Schiestl-Aalto et al. 2015, Hayat et al. 2017, Jones et al. 2020); these assumptions are implicit statements about NSC regulation, but their consequences are underexplored. Examining these implications may yield a useful shift in perspective.

To gain insight into how variations in NSC supply and demand result in observed NSC dynamics and the role of NSC regulation, we formulate NSC carbon mass balance in terms of concentrations. We derive a simple model for its conceptual utility, applicable to the analysis of experiments and more sophisticated models; the novelty of our approach is not detailed descriptions of component processes (see instead Thornley 1991;

Schiestl-Aalto et al. 2015, Hayat et al. 2017, Jones et al. 2020, Potkay et al. 2022) but techniques for describing how feedbacks govern NSC dynamics. A simple substrate dependence of demand on the amount of stored NSC is sufficient to regulate NSC dynamics. This simple regulation, in turn, permits complex NSC dynamics when the environmental changes.

To obtain practical insights, we analyze how seasonal starch dynamics vary under changes in seasonal photosynthesis (supply-driven seasonal dynamics) or changes in demand such as temperature-dependent seasonal variation in growth and respiration (demand-driven seasonal dynamics); we focus on starch under the assumption that sugar concentrations are regulated to remain near-constant. We demonstrate that each scenario creates a distinct seasonal variation in starch concentrations. We also demonstrate that peaks and valleys in seasonal dynamics lag imbalances in supply and demand; peaks and valleys represent moments when supply momentarily equals demand. Our results suggest that starch dynamics lag changes in carbon balance, but the degree of lag varies. Despite our focus on seasonal dynamics independent of plant size, our results suggest that more massive plants (mature trees) exhibit more lag and dampened starch dynamics when compared with less massive plants (saplings).

Methods

Theoretical framework

Three ideas form the basis of our approach. Beginning with a set of equations describing carbon mass balance: (i) expressing these equations in terms of concentrations scales NSC dynamics by plant size, approximately eliminating mass dynamics; (ii) effective feedbacks yield a single stable steady state in a constant environment, which implies that NSC concentrations affect the rates appearing carbon mass balance; and (iii) starch dynamics reflect changes in carbon balance, while sugar dynamics do not.

To explain the intuition for the mathematical framework, we begin with an analogy between NSC dynamics and the dynamics of water filling and draining from a bucket (Figure 1a). The change in NSC (change in water level) equals the rate of NSC supply (rate of inflow) minus the rate of NSC demand (rate of outflow) (Figure 1a). Expressing NSC dynamics in concentrations (idea 1) rather than absolute mass is analogous to expressing the amount of water as a fraction of the bucket's total capacity rather than the absolute amount of water. Environmental conditions influence the supply and demand rate such as adjustable valves whose changing aperture increases or decreases the conductance for flow in or out, modifying the flow rate but not necessarily determining it (Figure 1a). How the amount of NSC affects its supply and demand rate is analogous to how the amount of water affects the water pressure and, in turn, the inflow and outflow rates. When the environment is constant, a negative feedback between water level and net flow creates a stable steady state (Figure 1a) (idea 2). The nature of this feedback regulates the water level. As carbon mass balance applies to sugars, starch and total NSC, the analogy is applicable to either sugar or starch dynamics by a shift in interpretation.

We define NSC concentration as $s = y/m$ for a plant (or tissue) with y kg carbon of NSC and a total carbon mass of m kg. Differentiating this definition and rearranging provides a relationship between the change in NSC carbon concentrations $ds/dt = \dot{s}$ and changes in NSC carbon mass $\dot{y}$ and plant carbon mass $\dot{m}$ Eq. (1) (see supporting information Notes S2 available as Supplementary data at *Tree Physiology* Online). For ease of exposition, we will simply say NSC concentrations and plant biomass, rather than carbon biomass, because the resulting quantities have approximately the same value. Note that here again, y and s can be reinterpreted as the mass and concentration of either sugar or starch as the same definition applies to both.

$$\underbrace{\dot{s}}_{\text{change in [NSC]}} = \underbrace{\frac{\dot{y}}{m}}_{\text{net NSC change per mass}} - \underbrace{\frac{\dot{m}}{m}s}_{\text{[NSC] change from mass change}}. \quad (1)$$

Using our analogy (Figure 1a), the second term of the right-hand side Eq. (1) corresponds to how changes in bucket size affect the relative water amount, even though only the inflow and outflow affect the absolute amount of water. Although experiments report NSC concentrations as the fraction of NSC mass per dry biomass, theoretical or modeling papers sometimes use the fraction of NSC carbon mass per total carbon mass. We use the latter definition, because the former yields equations where the mass of nutrients (e.g., nitrogen, phosphorus, etc.) affects the NSC concentration, complicating equations; however, we show that the two definitions yield roughly similar values and have the same dynamics (see supporting information Notes S1 available as Supplementary data at *Tree Physiology* Online).

To obtain a useful description of dynamics, we insert rates of photosynthesis, respiration, growth and so on into Eq. (1). We then assume that respiration and growth rates vary as a function of NSC concentration s and combine all demands into a single demand term. To simplify, we linearize the demand about $s = 0$ yielding Eq. (2). See supporting information Notes S3 (available as Supplementary data at *Tree Physiology* Online) for full derivation.

$$\underbrace{\dot{s}}_{\text{change in NSC}} = \underbrace{A(1-s)}_{\text{supply}} - \underbrace{Us}_{\text{demand}}. \quad (2)$$

In Eq. (2), A is the specific rate of photosynthesis, or the mass of carbon assimilated per mass of carbon of plant mass

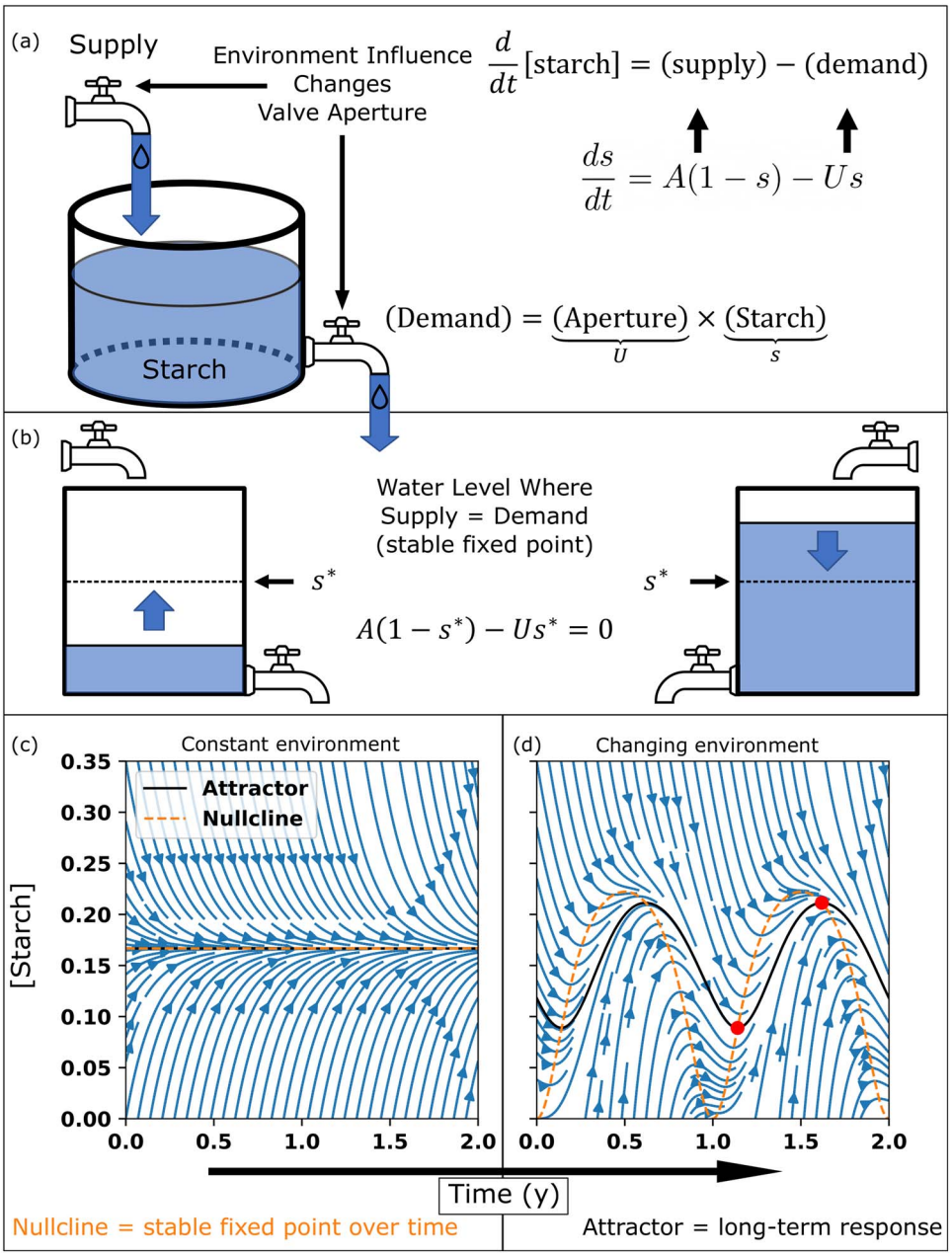

Figure 1. Nonstructural carbohydrate starch dynamics graphical derivation: dynamics analogous to water flowing in and out of a bucket where water level = [starch]; inflow rate = supply; outflow rate = demand; outflow valve aperture = usage rate (demand per unit starch); environment influences supply and demand rate by changing valve aperture (a). In constant environment, starch tends toward its stable fixed point (AKA steady state, equilibrium) at which the supply rate balances the demand rate (b). Streamplots (blue curves) show how simulated timeseries evolve from all starting positions under the same external drivers (c); the starch nullcline (dashed orange) is the path of the stable fixed point through time and indicates how the balance between supply and demand shift in time (c). All time-series quickly approach a long-term starch response called the attractor (solid black) (c); in a constant environment (left panel), the nullcline and attractor are constant in time and are equal, but in changing environments (right panel), the nullcline and attractor are no longer constant nor equal (c). Intersections (red points) between the nullcline and attractor always correspond to extrema (maxima or minima) of the attractor (c).

per unit time, while we call U the usage rate, derived as the linear coefficient from linearizing NSC demand. In this form, supply and demand rates are relative to plant mass. If the only demands are respiration and growth, then the usage rate is the rate of respiration plus growth in mass per unit mass of NSC. The usage rate U is the aperture of outflow valve, while demand is the rate of outflow (Figure 1a); it serves to quantify all other effects on demand beyond the feedback due to substrate dependence. This feedback is present virtually all models, past (Thornley 1970, Dewar 1993) and present (Thornley 2011, Schiestl-Aalto et al. 2015, Hayat et al. 2017, Jones et al. 2020). For that reason, this linearization may be applied to those models

to yield Eq. (2) with minor exceptions (e.g., Hayat et al. 2017 have respiration rates which do not depend on the amount of NSC stored). See additional discussion on the generality of this linearization in supporting information (see Notes S4 available as Supplementary data at *Tree Physiology* Online).

While a natural analogy for mass balance, our physical analogy (Figure 1a) goes beyond mass balance to include a feedback or regulation (water pressure regulates the net flow in and out). Mass balance is a simple and uncontroversial approach both for theoretical calculations or modeling (Thornley 1991; Landsberg and Waring 1997, Lacointe and Minchin 2008, Schiestl-Aalto et al. 2015, Jones et al. 2020) and for experimental estimates (Klein and Hoch 2015, Furze et al. 2019, Wiley et al. 2019). Mass balance does not preclude any dependence of NSC supply and demand on the amount of stored NSC, meaning that it is compatible with active and passive regulation of NSC, or even no regulation. The nature of regulation must refer to how stored NSC affects its supply and demand rate (i.e., how the blue streamlines in Figure 1c and d vary vertically). Some feedback must be present as without any feedback, NSC can 'overflow' or can become negative (i.e., some streamlines in Figure 1d would leave the range $0 \leq s \leq 1$). As these outcomes do not correspond to reality, they indicate a breakdown of a model; therefore, any good model must contain some feedback (i.e., all streamlines in Figure 1d cannot be the same and also remain within $0 \leq s \leq 1$). *A* thought experiment demonstrates the problem: assume a constant environment in which supply and demand only vary due to the feedback (e.g., Figure 1c rather than Figure 1d); in other words, we assume that the valve apertures do not change in time (but may be set to any value). In the analogy (Figure 1a), no feedback means that the net flow of water (supply minus demand) does not depend on water level, and therefore, the rate of change is constant; in other words, all streamlines (Figure 1c) are parallel lines. If positive, then the bucket fills forever (streamlines increase with time), and if negative, it drains forever (streamlines decrease with time). If zero, then no change occurs (horizontal streamlines). To exclude these possibilities, supply and demand must vary as a result of changes in NSC concentrations (i.e., the streamlines must vary vertically). Thus, at low NSC concentrations, supply exceeds demand, which prevents emptying, and at high NSC concentrations, demand exceeds supply, which prevents filling up (Figure 1b and c). As NSC concentrations increase or decrease (for each case, respectively), the rate of supply and demand change until a balance point occurs; at this concentration, supply equals demand and no further change occurs (Figure 1b and c). This balance point changes as the environment changes (Figure 1d), but its presence prevents model breakdown. This argument demonstrates that the amount of stored NSC must affect its own dynamics, but it does not mean that the amount of NSC is the only internal control regulating NSC dynamics. In fact, the addition of other internal controls is similar to a coupled system of sugar and starch dynamics. Other internal controls may mediate this feedback, but ultimately steady states require a feedback between the amount of NSC and its supply and demand.

Although playing distinct roles in carbon dynamics, growth and respiration have approximately the same effect on NSC whenever they collectively yield the same *U* rate. This 'lumping' approach to NSC demands is taken by other researchers, notably Thornley (2011) in the context of modeling respiration response (demand is termed *C* substrate utilization), Jones et al. (2020) in a simple NSC model for climate models (demand termed plant carbon expenditure) and Sala et al. (2012) in reviewing the role of NSC in carbon dynamics (demand termed *C* demand strength or *C* sink activity). While these studies and many whole-plant NSC models do not distinguish starch and sugar dynamics, Schiestl-Aalto et al. (2019) do present a whole-plant model with explicit differences in sugar and starch dynamics. Several models of phloem transport also contain explicit sugar and starch dynamics (e.g., Daudet et al. 2002; Lacointe and Minchin 2008, De Schepper and Steppe 2010).

To consider explicit sugar and starch dynamics, the picture in Figure 1a is modified to have two buckets, one for each pool. Instead of one, we have two mass balance equations (see details in Supplemental Information S5 available as Supplementary data at *Tree Physiology* Online), which include all processes affecting the amount of total NSC as well as the conversion between sugars and starch (starch synthesis and hydrolysis). While the combined system describes the coupled sugar and starch dynamics, we postulate that sugar dynamics do not reflect carbon balances. Sugar concentrations affect the osmotic pressure and sap viscosity of cells and surrounding tissues, in turn influencing cell hydration and phloem translocation (Talbott 1998, Secchi and Zwieniecki 2011, Woodruff and Meinzer 2011, Stroock et al. 2014, Woodruff 2014). Starch is not osmotically active in plants and can vary without affecting water balance or phloem transport. When illuminated, *Arabidopsis* leaves show starch accumulation while sugar concentrations remain constant, whereas *pgm* mutants, which cannot synthesize starch, show sugar accumulation instead (Gibon et al. 2004, Smith and Stitt 2007). These observations suggest that starch synthesis and hydrolysis keep sugar concentrations near a constant value, despite changes in photosynthesis, respiration, growth and transport affecting sugar concentrations, such that the overall effect is to pass carbon imbalance onto the starch pool. However, instead of assuming that sugar concentrations never vary, we make the subtler assumption that two timescales exist: a short timescale on which the coupled sugar and starch dynamics arrive at a steady state independent of carbon balance, and a long timescale on which changes in carbon balance change the coupled steady states. In terms of the bucket (Figure 1a), the sugar and starch buckets exchange water faster than water enters and exits the sugar bucket, so that the water level in either bucket is determined by the other at the long timescale due to the exchange in water

between buckets. The relationship between the two depends on how they exchange water (namely, the steady state of these dynamics), and we assume that it keeps sugar concentrations near a homeostatic value. If starch and sugar dynamics are so strongly coupled, then their dynamics may be expressed using only one of starch, sugar or total NSC since each formulation only reflects a change of coordinates. The technical term for this assumption is reduction to an approximate center manifold. Eq. (2) can then be formulated for any of the above and converted in between these; note that any feedbacks are also converted. Since we analyze seasonal dynamics below, we take the long timescale to be the same as seasonal dynamics (approximately a year) and the short timescale to be much shorter than that. Note that we assume that this timescale separation holds for simplicity, but given a system of sugar and starch dynamics, both the timescale and the relationship between sugar and starch concentrations can be computed. If starch synthesis and hydrolysis keep sugar concentrations near a certain value, then the variation in starch and total NSC will be almost the same (differing by the almost constant sugar concentrations). The same logic may be applied to NSC dynamics across various organs (roots, stems, leaves, etc.). If NSC translocation is faster than changes in carbon balance, then an average whole-plant NSC concentration contains sufficient information for dynamics at the long timescale, even if NSC concentrations are not uniform over the plant body. See supporting information Note S5 and Note S6 (available as Supplementary data at *Tree Physiology* Online) for additional discussion of these points. For the remainder of this article, we focus on starch dynamics for these reasons.

Analysis techniques

For NSC modeling, the novelty of our approach is not the detail of our model, but rather our mathematical analysis. We apply techniques from dynamical systems theory to describe the relationship between NSC regulation, dynamics and responses to the environment. We do our best to explain the principles of these techniques but recommend an excellent introductory text for readers seeking to apply these techniques (Strogatz 1994). See also Notes S4 (available as Supplementary data at *Tree Physiology* Online) in supporting information for an extended introduction and additional references Guckenheimer and Holmes (1983) and Wiggins (1996).

Starch dynamics in changing environments reflect the external forcing of a changing environment and the internal response of feedbacks. Streamplots (Figure 1c and d) are a geometric illustration of the *flow* of dynamics for Eq. (2); each blue curve shows the time evolution of starch concentrations from all possible starting conditions under the same time-series of A and U. Figure 1c shows a streamplot for a constant A and U, while Figure 1d shows a streamplot for time-varying A and U. Models with similar geometry in the streamplot will generate similar responses, even if their details, equations or parameterizations differ considerably; the geometry captures the essential properties of dynamics, the essential structure and how supply and demand rates vary as function of starch concentration determines the geometry.

If environmental conditions are constant, then A and U are constant (valve apertures are held at a constant). As shown in the thought experiment from the previous section (Figure 1b), all starch concentrations tend toward a balance point where supply equals demand (Figure 1c). Instead of balance point, this starch concentration is normally called a fixed point, steady state or equilibrium of Eq. (2). All trajectories or orbits from other initial starch concentrations converge on this value (Figure 1c). When the environment is constant, this fixed point is the long-term starch response, independent of the initial amount (Figure 1c). The fixed point is said to be stable, and in this case, the fixed point is the attractor for this system in a constant environment (Figure 1c). The attractor is the set of starch concentration toward which the system inevitably evolves at long timescales, independent of initial values. In a sense, the attractor is what one is most likely to measure in experiment. To calculate the fixed point s^* for a constant environment (Figure 1c), solve for zeros of Eq. (2).

$$\dot{s} = f\left(t, s^*\right) = A\left(1 - s^*\right) - Us^* = 0. \tag{3}$$

Eq. (2) has only one zero, hence a single fixed point. Eq. (2)'s simplicity makes direct calculation of the fixed point easy (cf. Jones et al. 2020 in supporting information S3 available as Supplementary data at *Tree Physiology* Online); the fixed point in a constant environment is given by Eq. (4)

$$s^* = \frac{A}{A+U}. \tag{4}$$

Plotting how the fixed point s^* varies as A and U vary demonstrates that external influences on supply and demand have nonlinear effects due to the feedbacks present (Figure 2).

While the fixed point indicates where starch concentrations converge in a constant environment (Figure 1c), the other important quantities is how quickly starch concentrations approach their fixed point. That rate of convergence can be estimated from the divergence of Eq. (2) ($\mathbf{div}\ \dot{s} = \partial\dot{s}/\partial s$) as the quantity r in Eq. (5).

$$r = A + U = -\frac{\partial \dot{s}}{\partial s}. \tag{5}$$

For brevity, we call r the response rate (also known as a Lyapunov exponent). Note that the response rate has unit dimension 1/time; alternatively, $\mathbf{log}(2)/r$ is a halving time (the approximate time needed to starch concentrations to half the distance to the fixed point). Higher rates of photosynthesis, respiration and growth imply higher response rates, lower halving times and thus faster convergence to the fixed point. Interesting timescale separations are possible when $r \ll 1$ (time-average methods) or $r \gg 1$ (quasi-steady state approximations).

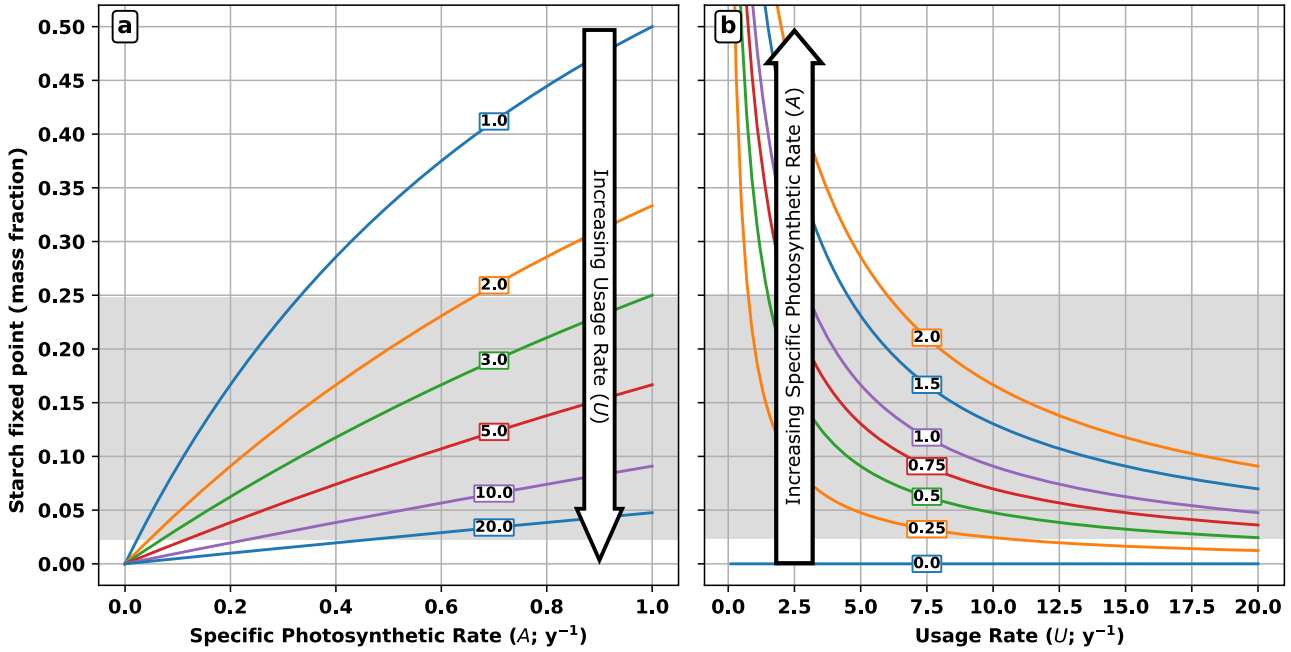

Figure 2. The starch fixed point (value of nullcline) increases with increasing specific photosynthetic rates A with constant usage rate U (a) but decreases with increasing usage rates U with constant specific photosynthetic rates A (b); numbers on each curve indicate the value of U in (a) or of $A\backslash$ in (b) held constant along the curve. Shaded range indicates typical values for NSCs.

The constant environment, with constant A and U, describes the feedback (Figure 1c), but changes in the environment change photosynthesis, respiration, growth and other processes causing the balance between supply and demand to shift (Figure 1d). As A or U change with time, no true fixed points exist; however, the existence of a stable fixed point for all possible environments implies that a stable long-term response exists. Solving equation (3) at each moment in time traces a curve in the starch-time plane (orange dashed curve in Figure 1c and d; black dashed curve in Figures 3–7) where the change in starch is momentarily zero; the slope is zero, and thus, we call this curve the starch null isocline (nullcline for short). As the environment changes, starch concentrations do not remain on the nullcline unlike a true fixed point; however, while it is not the actual starch response, the nullcline still represents the balance between supply and demand. Starch concentrations will tend toward a long-term response, an attractor (black curve in Figure 1d) determined by temporal variation in supply and demand and independent of the initial value, but not necessarily the nullcline (orange dashed curve in Figure 1d). As intuition, the nullcline indicates the direction in which NSC mass fractions will change (reflecting imbalances in supply and demand), the response rate measures the strength or timescale of those changes and the attractor is the long-term response. Short-term, transient responses quickly decay so the attractor represents the system's dynamics at long timescales and represents the cumulative recent history of supply and demand imbalances.

Effectively, changes in starch concentrations lag changes in the starch nullcline; the blue and black curves in the streamplot, which represent possible observable time-series, lag the nullcline (Figure 1d). The response may be dampened (smaller in magnitude). The lags and dampening occur because while nullcline reflects immediate changes in environmental conditions, these changes only become apparent in the starch time-series once sufficient accumulation or depletion has occurred. The relative difference between the response rate and the rate of change in the nullcline thus determines the degree of lag and dampening. Faster rates reduce the lag while slower rates increase the lag; this phenomenon is explored in simulations (Figures 1d and 3–7). The nullcline is a useful intermediate step in describing how variations in A and U push starch dynamics. Intersections between the nullcline and the attractor (or any time-series; both black and blue curves in Figures 1c and d, and 3–7) indicate whenever the imbalance in supply and demand switches sign; at this moment, supply and demand momentarily equal each other and this intersection always coincides with a local maximum or minimum (depending on the direction of intersection) of starch concentrations (e.g., red dots in Figure 1d; visible in Figures 3–7); by definition, the nullcline corresponds to starch concentration, where the slope (in starch-time plane) is zero. Even without any model, detecting maxima and minima in observed time-series indicates when starch dynamics switch between accumulation and depletion.

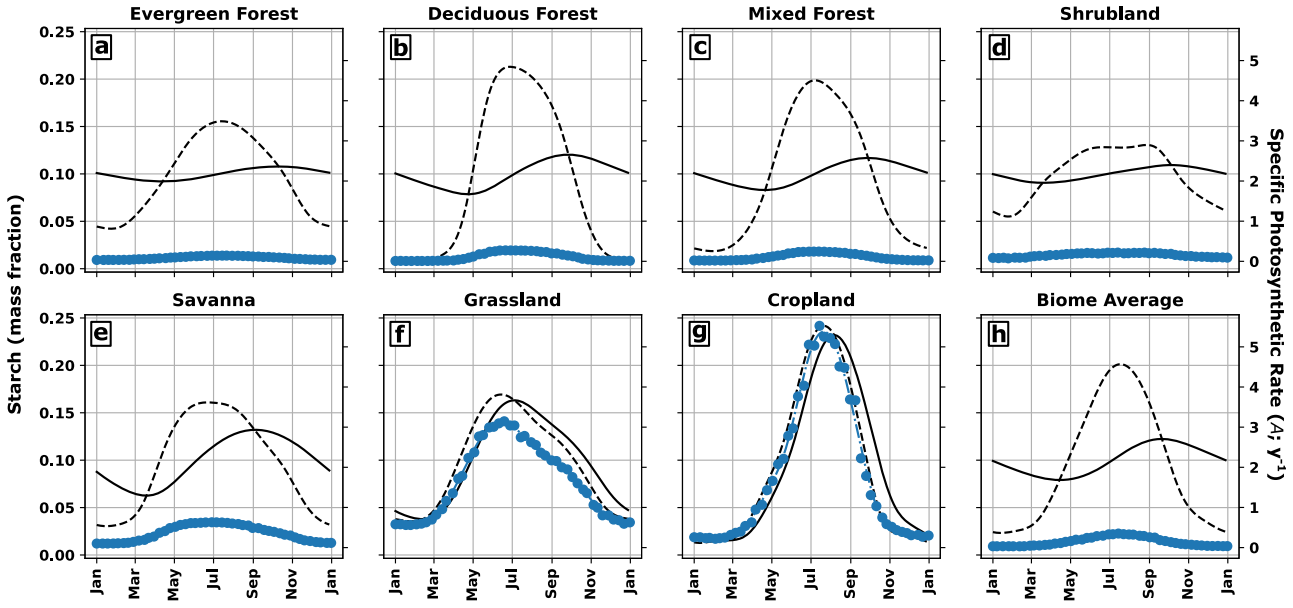

Figure 3. Seasonal variation in starch concentrations (solid black) and the starch nullcline (dashed black) assuming seasonal variation in specific photosynthetic rates (*A*, dash-dotted blue) only (supply-driven dynamics). The seasonal variation of *A* is based on GPP reported in Xiao et al. (2010) and ecosystem biomass reported in Saugier et al. (2001); dots indicate the data.

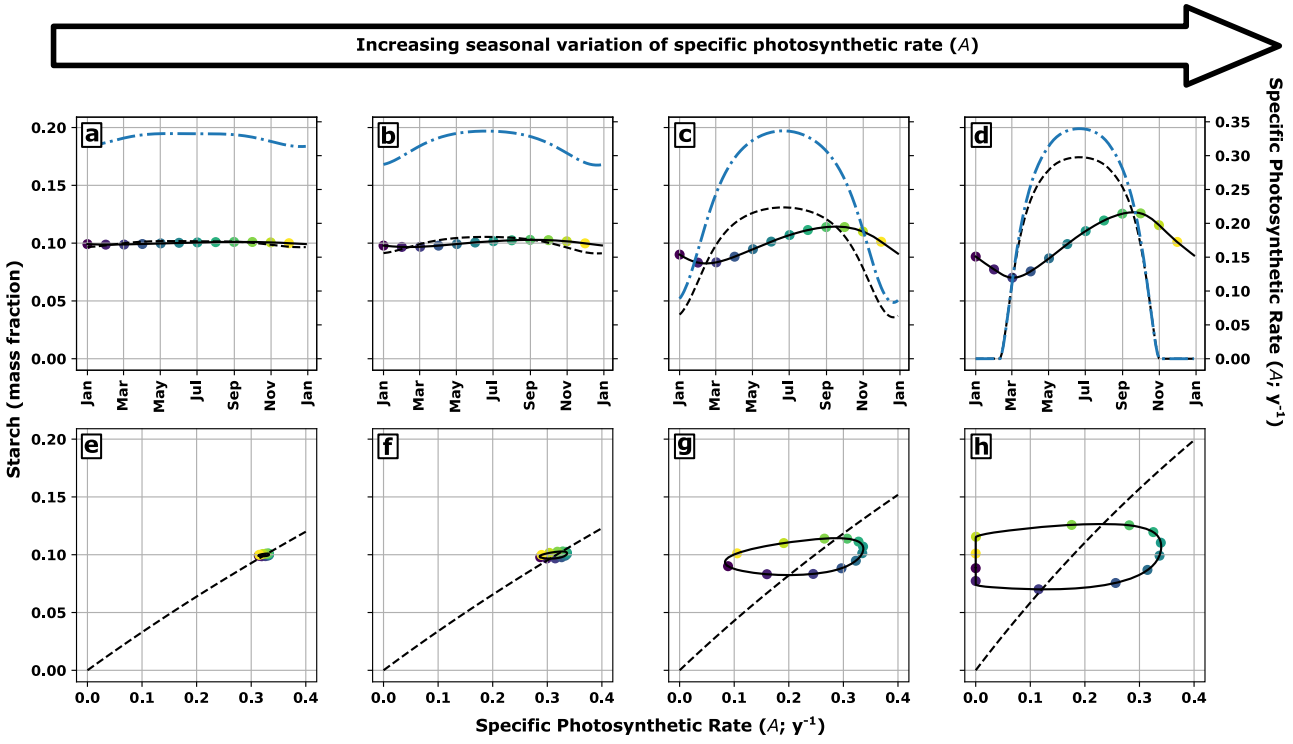

Figure 4. Seasonal variation in starch concentrations (solid black) and the starch nullcline (dashed black) assuming seasonal variation in specific photosynthetic rates (*A*, dash-dotted blue) only (supply-driven dynamics) by time-series (a–d) and bifurcation diagram (e–h); points on solid black curves indicate same time points; specific photosynthetic rates based on clear-sky seasonal light variation at latitudes 15°, 30°, 60° and 75° for (a–d) and (e–h), respectively.

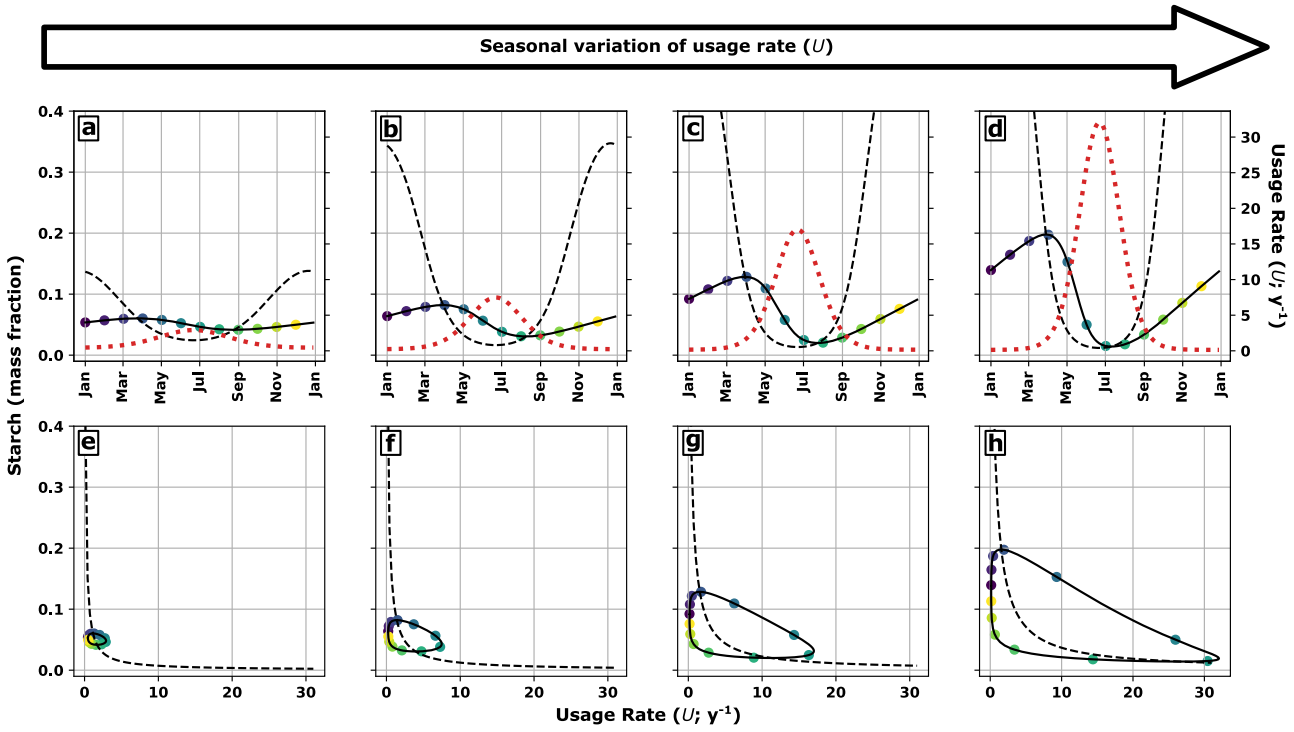

Figure 5. Seasonal variation in starch concentrations (solid black) and the starch nullcline (dashed black) assuming seasonal variation in usage rates (U, dotted red) only (demand-driven dynamics) by time-series (a–d) and bifurcation diagram (e–h). Points on solid black curves indicate same time points.

Application to seasonal NSC dynamics

Practical insight results from the application of these ideas to specific phenomena. To illustrate how starch dynamics respond to variations in A and U, we analyze possible seasonal starch dynamics using hypothetical seasonal variations in A and U in this article. We consider several scenarios: (i) seasonal variation in A drives starch dynamics, and U is constant (supply-driven dynamics); (ii) A is constant, and seasonal variation in U drives starch dynamics (demand-driven dynamics); (iii) A and U are synchronized (same timing of maximum; i.e., in phase); (iv) A and U are anti-synchronized (**max** U occurs 6 months before max A; i.e., 180° phase difference); and (v) U leads A (**max** U occurs 3 months before max **max** A; i.e., 90° phase difference). Note that in supply-driven dynamics, only supply is affected by external conditions but demand still varies, as demand depends on starch. Supply and demand both vary in all scenarios; we only change how the external environment influences the supply and demand rate. In analyzing seasonal dynamics, all simulations presented are based on Eq. (2) where the specific photosynthetic A and usage rate U are varied with time to simulate seasonal variation in photosynthesis and metabolic demand independent of NSC availability; the valves are constantly changed to modify the inflow and outflow rate (Figure 1a). Note that we focus on the response of starch dynamics rather than accurate simulation of photosynthetic, growth or respiration, for simplicity. Our goal is to describe how the starch dynamics respond to variation in photosynthetic, growth or respiration, and how feedbacks influence this response.

For periodic variations in A and U (i.e., seasonal variations), the nullcline and resulting attractor will also be periodic, while the transient responses are not periodic (Figure 1d); the streamlines (blue curves) are not periodic as they contain a transient response, while the attractor is periodic (black; Figure 1d), forming a closed loop in lower rows of Figures 4 and 5. Any idealization of seasonal dynamics must be periodic; otherwise, interannual feedbacks exist and the seasonal dynamics are transient. Likewise, the average seasonal dynamics will be periodic. For these reasons, we refer to the attractor as the starch concentrations one observes in the following unless otherwise noted. In Figures 3–7, we compute the nullcline and attractor and compare it with seasonal variations in A and U (direct computation method of the attractor in supporting information Notes S6 (available as Supplementary data at *Tree Physiology* Online), but a numerical integration method works as well). We suppress the transient responses (the blue curves in Figure 1d) for Figures 3–7 to avoid overcrowding.

For all scenarios, we assume that A and U have at most one annual maximum and one annual minimum (unless constant). Observations of gross primary production (GPP) (i.e.,

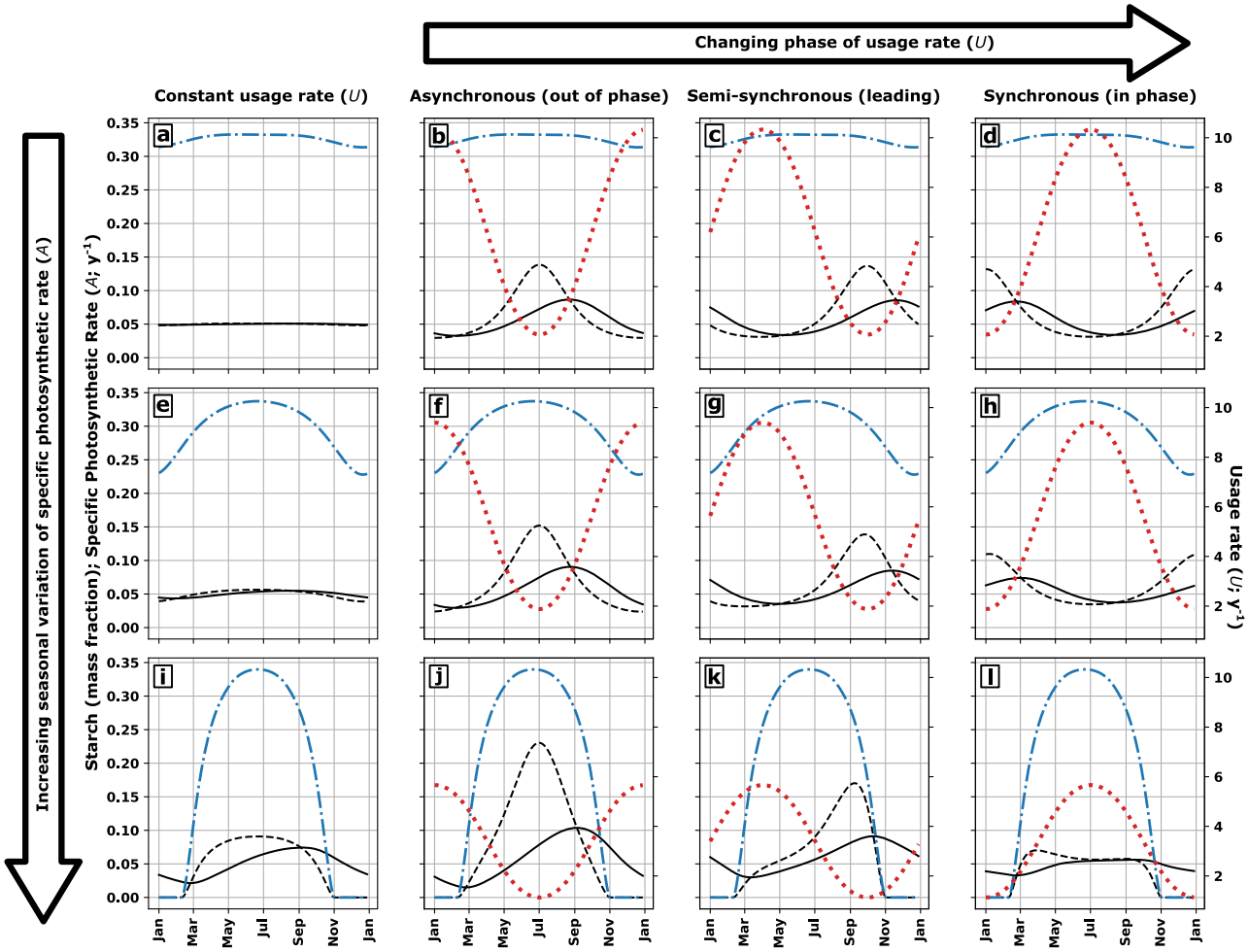

Figure 6. Seasonal variation in starch concentrations (solid black) and the starch nullcline (dashed black) when specific photosynthetic rates (A, dash-dotted blue) and usage rates (U, dotted red) are asynchronized with A and U out of phase (b, f, j), semi-synchronized with U leading A by 0.25 y (c, g, k), or synchronized with A and U in phase (d, h, l); seasonal variation with constant usage rate shown for comparison (a, e, i).

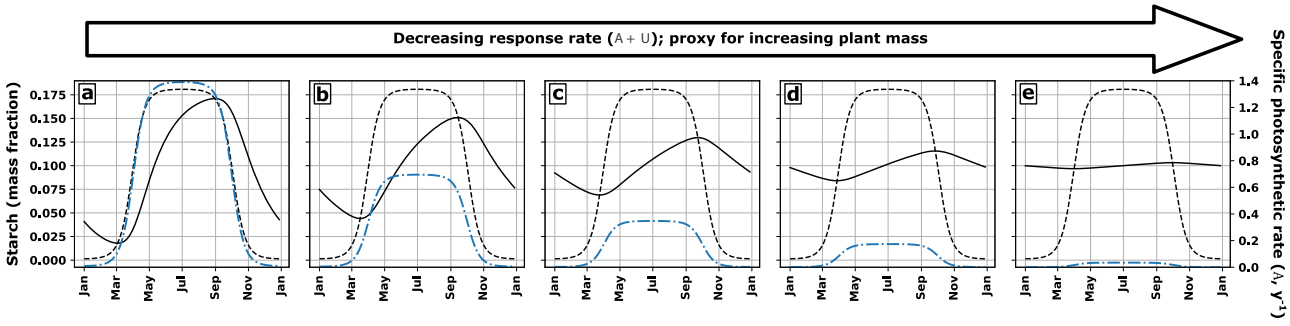

Figure 7. Seasonal variation in starch concentrations (solid black) with decreasing response rates $r = A + U$ (specific photosynthetic rate plus usage rate) but with the same starch nullcline (dashed black); variation in specific photosynthetic rates (dash-dotted blue) shown for comparison but a similar response is possible under variation in usage rate. Decreasing response rate corresponds to increasing plant mass (see text for explanation).

photosynthesis at ecosystem scale, proportional to A) are consistent with this assumption (Xiao et al. 2010), as are many starch time-series (Martínez-Vilalta et al. 2016). Similarly, we assume that variations in A and U on timescales much shorter than a year (i.e., daily variations) are averaged out and that variations are periodic, meaning that interannual variations at longer timescales are neglected. Our analysis of seasonal dynamics is simplified if starch dynamics are decoupled from plant mass dynamics; this approximation is valid if changes in plant biomass are small enough that seasonal A and U only

change due to the environment; this assumption should be accurate for sufficiently short timescales and for larger trees (see supporting information Note S8 available as Supplementary data at *Tree Physiology* Online). When valid, our analysis is mass-independent, the starch dynamics will be the same for plants of any size along if the specific photosynthetic and usage rates are the same.

To identify realistic seasonal variations in A for supply-driven dynamics, we simulated the variation in A by biome and by latitude. Biome seasonal variation in A was based on GPP observations, while latitude variations were based on light variation from solar position (more below). For demand-driven dynamics, we simulated seasonal changes in U to mimic the effect of seasonal temperature variation on growth and respiration. For synchronized and asynchronized dynamics, a combination was used. Our goal was to determine how A and U determine starch, rather than accurately model A or U responses (cf. Schiestl-Aalto et al. 2015). Specific biomes and latitudes illustrate, rather than predict, how A varies to aid interpretation of how starch dynamics respond to variation in A. We describe calculation details of specific seasonal variations in A and U in Methods S1 (available as Supplementary data at *Tree Physiology* Online) and only provide a brief overview here; however, the relevant variation in A and U is present when needed (Figures 3–7).

To determine reasonable magnitudes of A, we estimated average annual A using annual GPP and standing biomass estimates from Saugier et al. (2001) and Chapin et al. (2011) (see Table 6.6). We then determined reasonable seasonal variations of A using the observed seasonal variation in GPP across several different biomes in the continental USA based on satellite data (Xiao et al. 2010) and rescaled those observed GPP rates to match the average annual specific photosynthetic rate estimated for that biome. The values we use for specific photosynthetic rates are order-of-magnitude estimates. Estimating U independently is more difficult, requiring estimates of specific growth, respiration and litter production rates. Instead, we simply adjusted the magnitude of U so that the resulting starch concentrations would vary around 5–10%, a value consistent with measurements of starch. For demand-driven dynamics, the seasonal variation of U is designed to mimic a temperature-dependent enhancement (i.e., U increases as temperature increases) based on a Q10 exponential temperature response; the timing assumes a maximum near the summer solstice. For comparing asynchronized and synchronized dynamics, U switches smoothly between a high and low value to facilitate adjusting the amplitude and phase of U. Exact simulation details are provided in supporting information Methods S1. available as (Supplementary data at *Tree Physiology* Online)

Table 1 shows estimated annual average A for US biomes, while Figure 2 (in green) shows the observed seasonal variation in A (scaled to have the same average as the corresponding biome in Table 1). Specific photosynthetic rates A range plausibly 0—2 year^{-1}; $A = 0.2$ year^{-1} indicates the amount of carbon assimilated per year is 20% of total carbon biomass. Based on observations of starch concentrations, Eq. (2) implies that U typically will be greater than A with a ratio $U/A \approx (\mathbf{1} - \mathbf{s})/s$. To match observed starch concentrations ranging from 5 to 25%, U must range ~3–19 times greater than A.

Table 1. Ecosystem scale estimates of average annual specific photosynthetic rate (A; year^{-1}).

Biome	Specific photosynthetic rate (A)
Tropical forest	0.1238
Temperate forest	0.1124
Boreal forest	0.0855
Mediterranean shrubland	0.1563
Tropical savanna	0.3638
Temperate savanna	1.8403
Desert	0.7639
Tundra	0.5208
Cropland	2.0313

Results

As it forms a foundation for understanding simulation results, we begin our analysis by discussing how the starch fixed point or nullcline (Eq. 4) varies as specific photosynthetic rates A and usage rates U vary (Figure 2). Variations in the nullcline describes changes in the balance between A and U. As expected, increasing A increases supply pushing the fixed point toward higher starch concentrations (Figure 2a), while increasing U decreases demand pushing the fixed point toward lower starch concentrations (Figure 2b), assuming no other changes. In terms of concentrations, increases in NSC supply or demand have diminishing returns; for instance, doubling A would not quite double the fixed point of starch concentrations, and starch concentrations may be maintained under variations of A if U changes appropriately. Feedback creates the diminishing returns; changes in A instantaneously change supply but also indirectly change demand once sufficient time passes for starch to deplete or accumulate. The steady state respiration and growth rates are functions of photosynthesis (e.g., steady state demand is $Us^* = UA/(A + U)$), while they are unrelated for instantaneous changes. How source or sink limitations on growth affect NSC dynamics depends on whether limitations are transient or long-term.

Changes in starch concentration time-series will lag those in the starch nullcline as demonstrated in each simulation (Figures 3–7). Starch concentrations reach their seasonal maximum and minimum at intersections with the nullcline, indicating a switch in the net imbalance of supply and demand; therefore, starch concentrations do not necessarily reach their seasonal maximum and minimum during the summer and winter when

the nullcline is high and low (high and low imbalance), but instead during the spring and fall when the nullcline switches between its high and low value (imbalance switches sign). This phenomenon is present in all simulations (Figures 3–7), although the degree of lag depends on the response rate.

Scenario 1: supply-driven seasonal starch dynamics

If seasonal variation in A drives seasonal starch dynamics (supply-driven seasonal dynamics), then the resulting attractor of starch concentrations has one seasonal maximum (peak) and one seasonal minimum (valley) per year (Figures 3 and 4). Longer days in summer lead to higher average daily specific photosynthetic rates. High summertime photosynthesis corresponds to high starch nullcline. Starch concentrations increase in summer and decrease in winter. The seasonal maximum occurs in late summer or fall, while seasonal minimum occurs in spring or early summer when the net imbalance in supply and demand switches from positive to negative and vice versa (nullcline intersects attractor). The timing of these switches is the same across most biomes and latitudes because A oscillates between a high and low value (i.e., summer and winter) in these biomes and latitudes (Figures 3 and 4). The degree of lag varies from virtually no lag (croplands, Figure 3g) to about 3 months (deciduous forests, Figure 3b); the magnitude of A explains the degree of lag as the response rate $r = A + U$. Recall that U is constrained to give the same average starch concentrations. Changes in demand also lag supply as demand is proportional to starch concentrations.

As seasonal variation in annual A increases with latitude, seasonal variation in starch concentration increases (Figure 4). Increasing latitude increases the degree of variation in seasonal A but also reduces the overall average annual A (Figure 4). To keep average starch concentrations around 10%, U also decreases with latitude (but is still held constant); assuming the same U by latitude implies a decrease in average starch concentrations with latitude. In both cases, the decrease in specific photosynthetic rates results in a lower response rate indicating greater lag (Figure 4).

Scenario 2: demand-driven seasonal starch dynamics

Even if photosynthesis is constant, seasonal variation in growth and respiration (i.e., in U) also creates seasonal variation in NSC dynamics (demand-driven dynamics, scenario 2). If seasonal variation in U is highest in summer and lowest winter (to simulate temperature-dependent variation in sink activity), then the resulting attractor also has one seasonal maximum (peak) and one seasonal minimum (valley) per year but the timing is inverted (Figure 5). Demand is upregulated in summer, meaning that the nullcline is downregulated so that the nullcline's maximum occurs in winter (when U is lowest) rather than summer. Likewise, starch concentrations reach their maximum in spring or early summer rather than winter when the net imbalance in supply and demand switches from positive to negative and vice versa (nullcline intersects the attractor). Demand exceeds supply throughout summer. Although shifted in time, the timing of these maxima and minima is determined by the maxima and minima of the nullcline and the response rate; both of which depend on changes in U (cf. Figure 6b). For instance, if high summertime temperatures or low summertime water availability inhibited growth so that U was low in summer, then the maxima could be shifted forward by 6 months to be in late summer or fall as under supply-driven seasonal starch dynamics. Starch concentrations fall faster in summer than they increase in winter despite nullcline's symmetry because the response rate r is much higher in summer than winter (Figure 5). While the same phenomenon is present in supply-driven seasonal dynamics (Figure 4), to have the same amplitude in starch concentrations requires greater seasonal variation in U than seasonal A, making it more visible in demand-driven seasonal dynamics (Figure 5).

Scenarios 3–5: synchrony vs asynchrony in supply- and demand-driven starch dynamics

Outside of controlled experimental conditions, plants in most ecosystems would simultaneously experience changes in both A and U. Although the interaction of supply- and demand-driven dynamics could create many different seasonal patterns, we compare the effect of different degrees of synchrony (phase differences) between the seasonal variation of U and of A (Figure 6). Varying the amplitude changes the relative strength of A and U (Figure 6). When the environment influences both supply and demand, the resulting starch dynamics (Figure 6) fall between the general patterns of supply-driven (Figures 3 and 4) and demand-driven dynamics (Figure 5). When A varies little (simulating low latitudes), U (simulating sink activity) drives seasonal variation in starch concentrations which resemble demand-driven dynamics (Figure 5) but shifted in time depending on the timing of U (Figure 6a–d). Strong seasonal variation in A, especially zero wintertime A, can dominate seasonal variation in NSC mass fractions regardless of seasonal variation in growth and respiration; seasonal starch concentrations begin to resemble supply-driven seasonal dynamics (Figure 6j–l). Namely, even if reduced, demand still exceeds supply in winter because photosynthesis ceases in winter so any demand exceeds supply (Figure 6j–l). As a result, demand-driven dynamics may be more common at low latitudes, while supply-driven dynamics are typical at high latitudes, even within the same species (if its range is sufficiently large) or functional group (e.g., low latitude conifers vs high latitude conifers). Asynchrony in A and U strengthens the degree of seasonal variation in starch concentrations (Figure 6b, f and j), while synchrony weakens the seasonal variation (Figure 6d, h and l). High synchrony in A and U is likely in ecosystems with strong seasonality, but high synchrony dampens seasonal variation in starch dynamics. In many ecosystems, demand may be upregulated in spring before supply (e.g., growth onset leads leaf flush), suggesting some asynchrony.

Maxima and minima (peaks and valleys) in starch concentrations time-series indicate switches in the net imbalance between supply and demand; therefore, their timing provides a crude classification scheme for comparing synchronized and asynchronized supply and demand. Spring maxima and fall minima indicate demand exceeds supply in summer which can only occur when A remains high in winter relative to summertime with significant seasonal variation in U (sink activity) (Figure 6d and h). Fall maxima and spring minima indicate that supply exceeds demand in summer which occurs when either A in winter is zero or very low (Figure 6l) or A (source activity) and U (sink activity) are especially asynchronous (Figure 6b, f and j).

Discussion

In summary, we derived a simple dynamical system describing whole-plant starch dynamics, and we have demonstrated different patterns of seasonal starch dynamics result from variations in photosynthesis (A) and sink activity (U). We demonstrate several techniques for conceptualizing and analyzing NSC dynamics. Our simulations also illustrate that simple regulation may generate complex dynamics; while starch concentrations tend to a constant in a constant environment, an ever-changing environment causes starch concentrations to reflect the recent variations in that environment. We conclude with several relevant implications for NSC research.

First, our results provide insight into seasonal starch dynamics. Seasonal maxima and minima in starch concentrations indicate switches in the imbalance of supply and demand (Figures 3–7). Starch accumulates when supply exceeds demand and depletes when demand exceeds supply. As a result, peaks and valleys in starch concentration lags the maximum imbalance in supply and demand (i.e., the nullcline reflecting the balance point of supply and demand) and the degree of lag depends on the response rate (overall magnitude of supply and demand). Plants in latitudes and ecosystems without seasonal variations in photosynthesis, respiration and growth will not have seasonal variations in starch, a prediction consistent with Martínez-Vilalta et al. (2016) (cf. their Figure 6). Our results provide further theoretical support for the importance of detecting the timing of NSC minima and maxima, as suggested by Martínez-Vilalta et al. (2016); unfortunately, experimental observation of maxima and minima requires high-frequency measurements in addition to adequate sample sizes. The timing of extrema in supply-driven starch dynamics (minimum in spring, maximum in fall) appears typical for winter deciduous (cf. Figure 5 in Martínez-Vilalta et al. 2016, Tixier et al. 2020), while the timing of extrema in demand-driven dynamics (maximum in spring, minimum in fall) appears typical for conifers and evergreen angiosperms (cf. Figure 5 in Martínez-Vilalta et al. 2016, Aubrey and Teskey 2018, Oswald and Aubrey 2020); however, our simulations suggest that the typical timing of demand-driven dynamics will shift toward that of supply-driven dynamics as latitude increases (Figure 6d and l). High response rates (high photosynthesis and growth) lead to lower lag in starch concentrations, meaning a spring minimum and fall maximum shift toward a winter minimum and summer maximum in supply-driven dynamics. Thus, conifers at high latitudes (where photosynthesis is low or zero in winter) have summer or fall maxima in starch concentrations consistent with supply-driven dynamics (cf. Schoonmaker et al. 2021) rather than winter or spring minima in conifers at low latitudes exhibit demand-driven dynamics (cf. Aubrey and Teskey 2018, Oswald and Aubrey 2020). This switch suggests that photosynthesis can hide the influence of sink-limited growth and demand-related environmental influences; Blumstein and Hopkins (2021) make a similar observation: they find that a growth-storage tradeoff is only apparent after variation in photosynthesis is removed. While greater asynchrony in supply and demand would generate greater seasonal variation in starch dynamics, observations of photosynthesis, respiration and growth suggest that these processes are synchronized with a growing season at high latitudes; half-synchrony is equally plausible as growth rates may reach their maximum in spring, preceding the summertime high of photosynthesis and respiration, especially xylogenic growth precedes canopy leaf out. Our results suggest that seasonal dynamics may not reflect large seasonal asynchronies. Note that we have not made any assumptions regarding phenology beyond seasonal variations in photosynthesis, respiration and growth. Our analysis of seasonal starch dynamics complements the discussion by Piper (2021) in which a conceptual framework of how average non-structural carbon compound concentrations and its seasonal amplitude vary with growth rates. Independent measurements of respiration and growth rates would help constrain simulations, as U is harder to estimate in practice; models of sink-limited growth (e.g., Schiestl-Aalto et al. 2015) would also benefit from additional respiration and growth measurements.

Second, although our focus was seasonal dynamics, our framework is applicable to dynamics at other scales. For instance, a similar analysis of diurnal starch dynamics would complement our analysis of seasonal dynamics and provide insight into diurnal starch dynamics (Smith and Stitt 2007, Tixier et al. 2018, Gersony et al. 2020). Constant environment experiments simplify the application of our framework as A and U are constant. Constant light, shading or on–off photoperiod experiments are particularly amenable, especially when other factors such as temperature are held constant. To illustrate, suppose a complete shading experiment by assuming $A = 0$ and constant U; thus, Eq. (2) becomes $\dot{s} = -Us$ implying starch concentrations decay exponentially $s = s_0 e^{-Ut}$. Weber et al. (2018) observed this decay in whole-plant starch and sugar concentrations for *Acer pseudoplatanus*, *Quercus petraea*, *Picea*

abies and *Pinus sylvestris* in complete darkness. This result offers an the alternate interpretation to their experiment, suggesting that demands decreased exponentially as NSC ran out. When re-illuminated, starch concentrations then increase to the fixed point $A/(A+U)$ with the difference decaying exponentially at the response rate $r = A+U$. Weber et al. (2018) also observed this response, meaning that Eq. (2) describes the data using few parameters. Furthermore, comparing concentrations between different constant environments (i.e., controlled conditions of a growth chamber) would directly test the utility of Eq. (2).

Third, our calculations clarify the quantitative relationship between the dynamics of NSC mass and its concentration. Several authors have questioned if NSC concentrations indicate the degree of NSC 'storage' (Hoch 2015, Hartmann and Trumbore 2016); NSC mass and concentrations are equivalent—one can be converted to the other given total biomass—but while NSC mass tracks the absolute amount of NSC available for remobilization, concentrations measure remobilization relative to total mass. Photosynthesis and growth must also be expressed in relative terms; experimental observations confirm this relationship (Wiley et al. 2019).

Our calculations suggest that observed NSC dynamics on seedlings or saplings do not necessarily scale to mature canopy trees (Hartmann et al. 2018), as their response rates differ. To see why, we consider how seasonal starch dynamics change with plant mass. First, photosynthetic rates do not scale proportionally with plant mass, and therefore, specific photosynthetic rates vary with plant size. While photosynthesis and respiration rates increase in absolute size as plants grow larger, the rate relative to biomass shrinks; saplings might photosynthesize 1–3 times their total mass per (order-of-magnitude calculations), while mature canopy trees might only photosynthesize 0.1–0.5 times their total mass per year (Table 1). Self-shading decreases the marginal photosynthetic gain for new leaf area, while overall mass needed to support new leaf area increases faster than linearly; this decrease agrees with estimates based on allometric scaling (e.g., Enquist and Niklas 2002) and is present in process models such as the 3-PG model (Landsberg and Waring 1997, Landsberg and Sands 2011) where the specific photosynthetic rate scales as $A \propto \left(1-e^{-km}\right)/m$, tending to zero as mass increases (cf. Hayat et al. 2017). With constant U one expects decreasing starch concentrations; however, observations (Woodruff et al. 2004, Woodruff and Meinzer 2011) and several models (Hayat et al. 2017, Potkay et al. 2022) suggest that sink activity (measured by the usage rate U) also declines with increasing size. Thus, typical magnitudes of A, U, or both likely decrease as plant mass increases, leading to lower response rates for larger trees even if the nullcline is not affected.

To illustrate the effect on starch dynamics, consider the response rate $r = A + U$ changing with the same seasonal variation in the starch nullcline (Figure 7). High response rates mean supply and demand quickly come into balance with each other, due to high turnover of starch (Figure 7a and b), while low response rates mean supply and demand slowly come into balance with each other, due to low turnover (Figure 7d and e). As $r \to \infty$, starch concentrations become indistinguishable from the nullcline, while when $r \to 0$, starch concentrations do not respond to seasonal variations the nullcline because these variations are much too fast relative to the response rate. More massive trees would have smaller response rates than less massive ones and therefore have smaller seasonal amplitudes of starch as well as greater lag and dampening of responses. Alternatively, plants in poor, harsh environments having low photosynthetic and growth rates relative to total mass would also have smaller seasonal amplitudes and greater lag than fast-photosynthesizing, fast-growing counterparts. This argument suggests that tree mass is an important factor in analyzing of NSC dynamics, especially cross-study comparisons (cf. Martínez-Vilalta et al. 2016), and complements growth-storage tradeoff discussions (Piper 2021). Note that many studies on NSC dynamics do not report plant mass measurements (or estimates) at all; these measurements are necessary for determining not only whole-plant pool size but also response rates.

Our approach is limited in scope, but we believe that it contains promise for NSC research. Simply put, our simple model does not address dynamics that require multiple pools such as partitioning and spatial dynamics across the plant body. Typical observations reflect these dynamics in addition to seasonal carbon balance (e.g., Tixier et al. 2020, Davidson et al. 2021). Although often constant relative to starch dynamics, sugars do vary seasonally (Richardson et al. 2013, Schoonmaker et al. 2021); leaves, stems and roots often exhibit differences in NSC dynamics (Tixier et al. 2018; but see Schoonmaker et al. 2021). Our simple model and others (Schiestl-Aalto et al. 2015, Hayat et al. 2017; Jones et al. 2021) help identify what dynamics to expect by whole-plant carbon balance which in turn helps identify when measurements indicate other drivers. Furthermore, without modification, our derivation works for the mass balance of individual tissues. For instance, the bucket represents just leaf starch; supply becomes leaf photosynthesis and demand then reflects leaf carbon export in addition to growth and respiration. The interpretation shifts but the main ideas of our derivation, carbon mass balance and feedbacks generating a steady state, apply immediately. For instance, leaf starch concentrations should lag photosynthesis, and Gersony et al. (2020) observe maximum daily leaf starch concentration around 18:00 h in *Quercus*; they observe a lagging starch time-series to daily photosynthesis, similar to the supply-driven seasonal dynamics but at a daily timescale. *Arabidopsis* leaves also show the same pattern (Smith and Stitt 2007).

As discussed above, our analogy (Figure 1) extends to multiple NSC pools (including other compounds and individual

organs). The theoretical difficulty is not adding pools or processes, but rather specifying the necessary feedbacks or regulation of all processes (and their parameterization) and then analyzing how the individual pieces fit together. For instance, observed changes in sugar concentrations require assumptions beyond carbon dynamics to describe and are most likely related to xylem and phloem function (Jensen 2018, Sevanto 2018, Sapés et al. 2019, 2021). Spatial dynamics also depend heavily on phloem dynamics, not solely on whole-plant carbon balance. To improve models of NSC dynamics, detailed experimentation of phloem dynamics and the chemical kinetics of starch synthesis and hydrolysis would prove useful; however, the concepts of attractor, nullcline and response rate are applicable in models with more NSC pools and may prove useful for identifying the feedbacks (see supporting information Note S5–S6 available as Supplementary data at *Tree Physiology* Online). Here, we use such concepts to identify conditions under which more sophisticated models with explicit partitioning and spatial dynamics would simplify to our simple model, especially when certain timescale separations are present (see supporting information Note S5–Note S6 available as Supplementary data at *Tree Physiology* Online). Eq. (2) and other whole-plant models (e.g., Schiestl-Aalto et al. 2015, Hayat et al. 2017, Jones et al. 2020) remain valid approximations of whole-plant starch dynamics. Additional investigation is required to verify validity.

Lastly, our theoretical framework provides a new perspective on active and passive regulation as well as source and sink-limited plant growth. Regulation of NSC dynamics is a matter of feedback, of how photosynthesis, growth and respiration depend on the amount of NSC and not how they affect the rate of change in NSC, which is determined by mass balance. Whether photosynthesis, NSC or nutrients limit growth depends on the timescale; transient responses may differ from long-term responses (the attractor). For instance, at least one FACE experiment observed a transient growth increase that vanished at long timescales due to nitrogen limitation (Norby et al. 2010). The consequences of this shift in perspective merit further investigation in future works.

Data availability statement

Data sharing not applicable to this article as no datasets were generated or analyzed during the current study.

Supplementary data

Supplementary data for this article are available at *Tree Physiology* Online.

Conflict of interest

None declared.

Funding

This work was supported by the USDA National Institute of Food and Agriculture, Agriculture and Food Research Initiative McIntire Stennis project [1023985] and was based upon work supported by the US Department of Energy (DOE) to the University of Georgia Research Foundation [DE-EM0004391] and to the US Forest Service Savannah River [DE-EM0003622]. This material is also based upon work supported by the US Department of Energy, Office of Science, Office of Workforce Development for Teachers and Scientists, Office of Science Graduate Student Research (SCGSR) program. The SCGSR program is administered by the Oak Ridge Institute for Science and Education (ORISE) for the DOE. ORISE is managed by Oak Ridge Associated Universities (ORAU) under contract number [DE-SC0014664]. All opinions expressed in this paper are the authors' and do not necessarily reflect the policies and views of DOE, ORAU or ORISE.

Authors' contributions

S.W.O. developed the theory, wrote the manuscript and created the figures. D.P.A. edited and provided feedback on the manuscript and figures.

References

Ainsworth EA, Long SP (2005) What have we learned from 15 years of free-air CO_2 enrichment (FACE)? A meta-analytic review of the responses of photosynthesis, canopy properties and plant production to rising CO_2. New Phytol 165:351–372.

Arora VK, Boer GJ, Friedlingstein P et al. (2013) Carbon–concentration and carbon–climate feedbacks in CMIP5 earth system models. J Clim 26:5289–5314.

Aubrey DP, Teskey RO (2018) Stored root carbohydrates can maintain root respiration for extended periods. New Phytol 218:142–152.

Aubrey DP, Mortazavi B, O'Brien JJ, McGee JD, Hendricks JJ, Kuehn KA, Teskey RO, Mitchell RJ (2012) Influence of repeated canopy scorching on soil CO2 efflux. For Ecol Manage 282:142–148.

Blumstein M, Hopkins R (2021) Adaptive variation and plasticity in non-structural carbohydrate storage in a temperate tree species. Plant Cell Environ 44:2494–2505.

Bonan GB (2008) Forests and climate change: forcings, feedbacks, and the climate benefits of forests. Science 320:1444–1449.

Cannell MGR, Dewar RC (1994) Carbon allocation in trees: a review of concepts for modelling. In: M. Begon, A.H. Fitter Editor(s) Advances in ecological research. Academic Press, Elsevier, pp 59–104. https://linkinghub.elsevier.com/retrieve/pii/S0065250408602135 (21 September 2022, date last accessed).

Chapin FS, Schulze E, Mooney HA (1990) The ecology and economics of storage in plants. Annu Rev Ecol Syst 21:423–447.

Chapin FS, Matson PA, Vitousek PM (2011) Principles of terrestrial ecosystem ecology, 2nd edn. Springer, New York.

Collins AD, Ryan MG, Adams HD, Dickman LT, Garcia-Forner N, Grossiord C, Powers HH, Sevanto S, McDowell NG (2021) Foliar respiration is related to photosynthetic, growth and carbohydrate response to experimental drought and elevated temperature. Plant Cell Environ 44:3853–3865.

Daudet F, Lacointe A, Gaudillère J, Cruiziat P (2002) Generalized Münch Coupling between Sugar and Water Fluxes for Modelling Carbon Allocation as Affected by Water Status. Journal of Theoretical Biology 214(3), 481–498..

Davidson AM, Le ST, Cooper KB, Lange E, Zwieniecki MA (2021) No time to rest: seasonal dynamics of non-structural carbohydrates in twigs of three Mediterranean tree species suggest year-round activity. Sci Rep 11:5181.

De Schepper V, Steppe K (2010) Development and verification of a water and sugar transport model using measured stem diameter variations. J Exp Bot 61:2083–2099.

Dewar RC (1993) A root-shoot partitioning model based on carbon-nitrogen-water interactions and munch phloem flow. Funct Ecol 7:356.

Dietze MC, Sala A, Carbone MS, Czimczik CI, Mantooth JA, Richardson AD, Vargas R (2014) Nonstructural carbon in woody plants. Annu Rev Plant Biol 65:667–687.

Enquist BJ, Niklas KJ (2002) Global allocation rules for patterns of biomass partitioning in seed plants. Science 295:1517–1520.

Epstein E (1971) Mineral nutrition of plants: principles and perspectives. Wiley, New York.

Epstein E, Bloom AJ (2005) Mineral nutrition of plants: principles and perspectives, 2nd edn. Sinauer Associates, Sunderland, MA.

Farquhar GD, von Caemmerer S, Berry JA (1980) A biochemical model of photosynthetic CO2 assimilation in leaves of C3 species. Planta 149:78–90.

Fatichi S, Leuzinger S, Körner C (2014) Moving beyond photosynthesis: from carbon source to sink-driven vegetation modeling. New Phytol 201:1086–1095.

Fatichi S, Pappas C, Zscheischler J, Leuzinger S (2019) Modelling carbon sources and sinks in terrestrial vegetation. New Phytol 221:652–668.

Franklin O, Johansson J, Dewar RC, Dieckmann U, McMurtrie RE, Brannstrom A, Dybzinski R (2012) Modeling carbon allocation in trees: a search for principles. Tree Physiol 32:648–666.

Friedlingstein P, Meinshausen M, Arora VK, Jones CD, Anav A, Liddicoat SK, Knutti R (2014) Uncertainties in CMIP5 climate projections due to carbon cycle feedbacks. J Clim 27:511–526.

Furze ME, Huggett BA, Aubrecht DM, Stolz CD, Carbone MS, Richardson AD (2019) Whole-tree nonstructural carbohydrate storage and seasonal dynamics in five temperate species. New Phytol 221:1466–1477.

Gersony JT, Hochberg U, Rockwell FE, Park M, Gauthier PPG, Holbrook NM (2020) Leaf carbon export and nonstructural carbohydrates in relation to diurnal water dynamics in mature oak trees. Plant Physiol 183:1612–1621.

Gibon Y, Bläsing OE, Palacios-Rojas N, Pankovic D, Hendriks JHM, Fisahn J, Höhne M, Günther M, Stitt M (2004) Adjustment of diurnal starch turnover to short days: depletion of sugar during the night leads to a temporary inhibition of carbohydrate utilization, accumulation of sugars and post-translational activation of ADP-glucose pyrophosphorylase in the following light period. Plant J 39: 847–862.

Guckenheimer J, Holmes P (1983) Nonlinear oscillations, dynamical systems, and bifurcations of vector fields. Springer New York, New York, NY. http://link.springer.com/10.1007/978-1-4612-1140-2 (21 September 2022, date last accessed).

Hartmann H, Trumbore S (2016) Understanding the roles of nonstructural carbohydrates in forest trees – from what we can measure to what we want to know. New Phytol 211:386–403.

Hartmann H, Adams HD, Hammond WM, Hoch G, Landhäusser SM, Wiley E, Zaehle S (2018) Identifying differences in carbohydrate dynamics of seedlings and mature trees to improve carbon allocation in models for trees and forests. Environ Exp Bot 152:7–18.

Hartmann H, Bahn M, Carbone M, Richardson AD (2020) Plant carbon allocation in a changing world – challenges and progress: introduction to a virtual issue on carbon allocation: introduction to a virtual issue on carbon allocation. New Phytol 227:981–988.

Hayat A, Hacket-Pain AJ, Pretzsch H, Rademacher TT, Friend AD (2017) Modeling tree growth taking into account carbon source and sink limitations. Front Plant Sci 8. https://doi.org/10.3389/fpls.2017.00182.

Hoch G (2015) Carbon reserves as indicators for carbon limitation in trees. In: Lüttge U, Beyschlag W (eds) Progress in botany. Springer International Publishing, Cham, pp 321–346. http://link.springer.com/10.1007/978-3-319-08807-5_13 (13 April 2022, date last accessed).

Högberg P, Nordgren A, Buchmann N, Taylor AFS, Ekblad A, Högberg MN, Nyberg G, Ottosson-Löfvenius M, Read DJ (2001) Large-scale forest girdling shows that current photosynthesis drives soil respiration. Nature 411:789–792.

Jensen KH (2018) Phloem physics: mechanisms, constraints, and perspectives. Curr Opin Plant Biol 43:96–100.

Jones S, Rowland L, Cox P et al. (2020) The impact of a simple representation of non-structural carbohydrates on the simulated response of tropical forests to drought. Biogeosciences 17:3589–3612.

Klein T, Hoch G (2015) Tree carbon allocation dynamics determined using a carbon mass balance approach. New Phytol 205:147–159.

Körner C (2003) Carbon limitation in trees. J Ecol 91:4–17.

Körner C (2015) Paradigm shift in plant growth control. Curr Opin Plant Biol 25:107–114.

Kozlowski TT (1992) Carbohydrate sources and sinks in woody plants. Bot Rev 58:107–222.

Lacointe A, Minchin PEH (2008) Modelling phloem and xylem transport within a complex architecture. Funct Plant Biol 35:772.

Landsberg J (2003) Modelling forest ecosystems: state of the art, challenges, and future directions. Can J For Res 33:385–397.

Landsberg JJ, Sands PJ (2011) Physiological ecology of forest production: principles, processes and models, 1st edn. Academic Press/Elsevier, Amsterdam, Boston.

Landsberg JJ, Waring RH (1997) A generalised model of forest productivity using simplified concepts of radiation-use efficiency, carbon balance and partitioning. For Ecol Manage 95:209–228.

Le Roux X, Lacointe A, Escobar-Gutiérrez A, Le Dizés S (2001) Carbon-based models of individual tree growth: a critical appraisal. Ann For Sci 58:469–506.

Leuzinger S, Manusch C, Bugmann H, Wolf A (2013) A sink-limited growth model improves biomass estimation along boreal and alpine tree lines: sink limitation in vegetation modelling. Glob Ecol Biogeogr 22:924–932.

Lovenduski NS, Bonan GB (2017) Reducing uncertainty in projections of terrestrial carbon uptake. Environ Res Lett 12:044020.

Ma S, He F, Tian D et al. (2018) Variations and determinants of carbon content in plants: a global synthesis. Biogeosciences 15:693–702.

Martínez-Vilalta J, Sala A, Asensio D, Galiano L, Hoch G, Palacio S, Piper FI, Lloret F (2016) Dynamics of non-structural carbohydrates in terrestrial plants: a global synthesis. Ecol Monogr 86: 495–516.

Norby RJ, Warren JM, Iversen CM, Medlyn BE, McMurtrie RE (2010) CO_2 enhancement of forest productivity constrained by limited nitrogen availability. Proceedings of the National Academy of Sciences 107(45), 19368–19373.

Norby RJ, Zak DR (2011) Ecological lessons from free-air CO_2 enrichment (FACE) experiments. Annu Rev Ecol Evol Syst 42:181–203.

Nowak RS, Ellsworth DS, Smith SD (2004) Functional responses of plants to elevated atmospheric CO_2 – do photosynthetic and productivity data from FACE experiments support early predictions? New Phytol 162:253–280.

Oswald SW, Aubrey DP (2020) Xeric tree populations exhibit delayed summer depletion of root starch relative to Mesic counterparts. Forests 11:1026.

Piper FI (2021) Putting non-structural compounds on the map of plant life history strategies: a commentary on Schoonmaker et al.. Tree Physiol 41:1559–1562.

Potkay A, Hölttä T, Trugman AT, Fan Y (2022) Turgor-limited predictions of tree growth, height and metabolic scaling over tree lifespans. Tree Physiol 42:229–252.

Quetin GR, Swann ALS (2018) Sensitivity of leaf area to interannual climate variation as a diagnostic of ecosystem function in CMIP5 carbon cycle models. J Clim 31:8607–8625.

Richardson AD, Carbone MS, Keenan TF, Czimczik CI, Hollinger DY, Murakami P, Schaberg PG, Xu X (2013) Seasonal dynamics and age of stemwood nonstructural carbohydrates in temperate forest trees. New Phytol 197:850–861.

Ruswick SK, O'Brien JJ, Aubrey DP (2021) Carbon starvation is absent regardless of season of burn in *Liquidambar styraciflua* L. For Ecol Manage 479:118588.

Sala A, Woodruff DR, Meinzer FC (2012) Carbon dynamics in trees: feast or famine? Tree Physiol 32:764–775.

Sapés G, Roskilly B, Dobrowski S, Maneta M, Anderegg WRL, Martinez-Vilalta J, Sala A (2019) Plant water content integrates hydraulics and carbon depletion to predict drought-induced seedling mortality. Tree Physiol 39:1300–1312.

Sapés G, Demaree P, Lekberg Y, Sala A (2021) Plant carbohydrate depletion impairs water relations and spreads via ectomycorrhizal networks. New Phytol 229:3172–3183.

Saugier B, Roy J, Mooney HA (2001) 23 - Estimations of global terrestrial productivity: Converging toward a single number? In: Jacques Roy, Bernard Saugier, Harold A. Mooney Editor(s) Physiological Ecology, Terrestrial Global Productivity. Academic Press, pp 543–557. https://linkinghub.elsevier.com/retrieve/pii/B9780125052900500247 (13 April 2022, date last accessed).

Schiestl-Aalto P, Kulmala L, Mäkinen H, Nikinmaa E, Mäkelä A (2015) CASSIA – a dynamic model for predicting intra-annual sink demand and interannual growth variation in Scots pine. New Phytol 206:647–659.

Schiestl-Aalto P, Ryhti K, Mäkelä A, Peltoniemi M, Bäck J, Kulmala L (2019) Analysis of the NSC storage dynamics in tree organs reveals the allocation to belowground symbionts in the framework of whole tree carbon balance. Front For Glob Change 2:17.

Schoonmaker AL, Hillabrand RM, Lieffers VJ, Chow PS, Landhäusser SM (2021) Seasonal dynamics of non-structural carbon pools and their relationship to growth in two boreal conifer tree species. Tree Physiol 41:1563–1582.

Secchi F, Zwieniecki MA (2011) Sensing embolism in xylem vessels: the role of sucrose as a trigger for refilling: sensing embolism in poplar vessels. Plant Cell Environ 34:514–524.

Sevanto S (2018) Drought impacts on phloem transport. Curr Opin Plant Biol 43:76–81.

Sevanto S, Mcdowell NG, Dickman LT, Pangle R, Pockman WT (2014) How do trees die? A test of the hydraulic failure and carbon starvation hypotheses. Plant Cell Environ 37:153–161.

Smith AM, Stitt M (2007) Coordination of carbon supply and plant growth. Plant Cell Environ 30:1126–1149.

Strogatz SH (1994) Nonlinear dynamics and chaos: with applications to physics, biology, chemistry, and engineering. Addison-Wesley publ, Reading, MA.

Stroock AD, Pagay VV, Zwieniecki MA, Michele Holbrook N (2014) The physicochemical hydrodynamics of vascular plants. Annu Rev Fluid Mech 46:615–642.

Talbott L (1998) The role of sucrose in guard cell osmoregulation. J Exp Bot 49:329–337.

Thornley JHM (1970) Respiration, growth and maintenance in plants. Nature 227:304–305.

Thornley JHM (1971) Energy, respiration, and growth in plants. Ann Bot 35:721–728.

Thornley JHM (1972) A balanced quantitative model for root: shoot ratios in vegetative plants. Ann Bot 36:431–441.

Thornley JHM (1991) A transport-resistance model of forest growth and partitioning. Annals of Botany 68(3), 211–226.

Thornley JHM (2011) Plant growth and respiration re-visited: maintenance respiration defined – it is an emergent property of, not a separate process within, the system – and why the respiration : photosynthesis ratio is conservative. Ann Bot 108: 1365–1380.

Tixier A, Orozco J, Roxas AA, Earles JM, Zwieniecki MA (2018) Diurnal variation in nonstructural carbohydrate storage in trees: remobilization and vertical mixing. Plant Physiol 178:1602–1613.

Tixier A, Guzmán-Delgado P, Sperling O, Amico Roxas A, Laca E, Zwieniecki MA (2020) Comparison of phenological traits, growth patterns, and seasonal dynamics of non-structural carbohydrate in Mediterranean tree crop species. Sci Rep 10:347.

Von Caemmerer S (2013) Steady-state models of photosynthesis: steady-state models of photosynthesis. Plant Cell Environ 36:1617–1630.

Weber R, Schwendener A, Schmid S, Lambert S, Wiley E, Landhäusser SM, Hartmann H, Hoch G (2018) Living on next to nothing: tree seedlings can survive weeks with very low carbohydrate concentrations. New Phytol 218:107–118.

Wiggins S (1996) Introduction to applied nonlinear dynamical systems and chaos, Corr. 3rd print. Springer, New York.

Wiley E, Helliker B (2012) A re-evaluation of carbon storage in trees lends greater support for carbon limitation to growth. New Phytol 195:285–289.

Wiley E, King CM, Landhäusser SM (2019) Identifying the relevant carbohydrate storage pools available for remobilization in aspen roots tissue D (ed). Tree Physiol 39:1109–1120.

Woodruff DR (2014) The impacts of water stress on phloem transport in Douglas-fir trees. Tree Physiol 34:5–14.

Woodruff DR, Meinzer FC (2011) Water stress, shoot growth and storage of non-structural carbohydrates along a tree height gradient in a tall conifer: growth, water stress and carbohydrate storage. Plant Cell Environ 34:1920–1930.

Woodruff DR, Bond BJ, Meinzer FC (2004) Does turgor limit growth in tall trees? Plant Cell Environ 27:229–236.

Xiao J, Zhuang Q, Law BE, Chen J, Baldocchi DD, Cook DR, Oren R, Richardson AD, Wharton S, Ma S (2010) A continuous measure of gross primary production for the conterminous United States derived from MODIS and AmeriFlux data. Remote Sens Environ 114:576–591.